Wireless Networks 7, 173–185, 2001

The Impact of Mobility on Cellular Network Configuration

BEZALEL GAVISH
Cox School of Business, Southern Methodist University, Dallas, TX 75275-0333, USA

SURESH SRIDHAR
I2 Technologies, 909 E. Las Colinas Blvd., Irving, TX 57039, USA

Abstract. This paper proposes a model for configuring cellular networks to study the dynamics of mobility between a single cell and its adjacent cells. It differs from most models considered in the literature by explicitly incorporating the dependency between the handoff rate and the system state. Besides, the handoff rate is also a function of cell size and subscriber mobility. Extensive computational experiments were done to study the impact of various input parameters on specific performance measures. Several observations are made regarding the system performance and as to how they are affected by the complex interaction between subscriber mobility, cell size, number of channels and the mean call initiation rate. The results of these experiments show that the proposed model, where handoff rates are state-dependent, captures additional traffic due to mobility when compared to the traditional method of modeling handoffs using information about the average behavior. Finally, the economic impact of mobility on system configuration decisions is analyzed. Though an approximation, the above work provides interesting insights about the impact of mobility in configuring cellular networks.

Keywords: cellular networks, configuration, economics, mobility

1. Introduction

Cellular radio networks are one of the fastest growing segments in the communications industry. The average annual growth rate has varied from 40 to 60% worldwide. This surge in demand has spurred tremendous research interest in this field.

A cellular radio network consists of several cells covering a service area. Each cell has a base station which serves the subscribers in its vicinity. The subscribers may be either stationary or mobile. Each base station is assigned a specific number of channels, each of which can accommodate one or more calls depending on the transmission and encoding technology (e.g., FDMA, TDMA, or CDMA).

One of the major features of a cellular network, in contrast to a traditional public switched telephone network, is subscriber mobility. This implies that when a subscriber moves from one cell to another, the call in progress has to be handed off from one base station to another to ensure continuity of service. If no channels are available in the adjacent cell, then the call might be interrupted and dropped. Call handoff rate and handoff policies have several implications, for example, on the number of channels assigned to a cell, the quality of service, and the expected net revenue.

Several models have been proposed in the literature to address the impact of mobility on system performance. Some of the major differences among these models are in terms of channel assignment [10,14], priority given to handoff calls [1,11], use of overlap between cells [9], mobility pattern with respect to speed and direction [6,8,13], multiple handoffs [16] and use of overlaying cells [7,17].

One of the interesting features of mobility is that the rate of handoff calls to a given cell depends on the number of calls in progress in the adjacent cells. Thus, assuming that subscriber mobility remains unchanged, an increase in the number of calls in adjacent cells is likely to increase the rate at which calls are handed off to the given cell. This implies that the handoff rate is a function of the system state. In that respect, the model proposed in this paper differs from most models considered in the literature by explicitly incorporating the dependency between the handoff rate in adjacent cells and the system state (in terms of number of calls in progress). Another difference is that unlike many models, the handoff rate is also a function of the cell size and the speed of movement of the subscriber. This model is used to study the dynamics between a single cell and its adjacent cells. It builds upon an earlier model [4] but extends it to explicitly account for subscriber mobility.

The paper is organized as follows. In section 2, the approach used to model handoff rates, which distinguishes this work from most of the previous work in this area, is described. The assumptions and notation used in the model are presented in section 3. A description of the model along with its analysis are given in sections 4 and 5, respectively. In section 6, the steps used to determine the performance measures of interest to the system designer are presented. The details of the computational experiments are described in section 7 and the results are summarized in section 8. These results are compared with those obtained using the traditional method of modeling handoffs in section 9. Finally, the economic implications of mobility are discussed in section 10.

2. Handoff rates

One of the methods used in the literature for modeling handoffs is to use information about the average behavior. For ex-

ample, if a cellular network is modeled as an open network of queues, the handoff attempts are modeled approximately by assuming a fixed probability θ_{ij} of call transitions from cell i to cell j [2,11]. Let $\rho_j = e_j/(\eta + \mu)$, where η is the handoff rate per ongoing call, μ is the mean rate of call completion per call, and e_j is the total arrival rate of new calls and handoff calls to cell j. Let λ_j denote the mean arrival rate of new calls in cell j. Let B_j denote the blocking probability of calls in cell j given by

$$B_j = E(\rho_j, C_j), \tag{1}$$

where C_j is the number of channels in cell j and $E(\cdot,\cdot)$ is the Erlang loss function. Then, under equilibrium conditions,

$$e_i = \lambda_i + \sum_j (1 - B_j) e_j \theta_{ji}. \tag{2}$$

A major advantage of the above method is that it is simple to model. It considers the call transitions between cells based on the average values. However, it does not explicitly capture the effect of state changes within a cell. Clearly, the state changes within a cell influence the blocking of new calls as well as handoff calls, and also determine the rate at which calls are handed off to other cells.

A different method that can be used to model handoffs is to consider the channel usage in each cell at any instant. This is similar to the concept used in an $M/M/c/c$ queue where the service rate varies directly with the number of busy servers [5]. Thus, if $1/\mu$ is the mean of the service-time distribution of each server, then the total service rate is $k\mu$ for $1 \leqslant k \leqslant c$ and 0 otherwise. The above concept can be extended to handoff rates as well. Thus, the outgoing handoff rate from a cell varies as a linear function of the number of calls in progress in the cell. The corresponding model is expected to be more accurate than the one based on the average behavior.

A model using an idea similar to the state-dependent method has been proposed in the context of dynamic channel allocation [14]. However, it is based on a rather unrealistic assumption that blocked handoffs are not cleared from the system; instead they remain in their current cell. Besides, dynamic channel allocation is more difficult to implement than fixed channel allocation. In this paper, the state-dependent method is used to model handoffs. It is assumed that blocked calls are cleared and that fixed channel allocation is used. The results of the computational experiments using this approach are then compared with those obtained from the first method.

3. Assumptions and notation

The major assumptions used in the model are stated below.

1. The cellular network is homogeneous (i.e., cells are symmetric in terms of size, shape, number of channels allocated, etc.).
2. Fixed channel allocation is used.
3. Demand is uniformly distributed in the given service area.
4. Both new calls and handoff calls are treated alike (i.e., neither type of calls is given priority over the other).
5. New call arrivals follow a Poisson process.
6. Unencumbered call duration (i.e., call duration assuming that the call is completed) is exponentially distributed.
7. The overlap between cells is negligible relative to the cell size.
8. Each cell is big enough so that the number of active calls does not affect the mean call initiation rate in that cell.
9. Subscriber residual time (i.e., the time spent in a cell by the subscriber associated with a successful call) is exponentially distributed.
10. Each subscriber is assumed to move at a random speed and an independent moving direction uniformly distributed in $(0, 2\pi)$.

The above assumptions are common in the literature on cellular networks (e.g., [1,2,4,10,23]).

The notation used in the model is given below. Additional notation is defined in the appropriate sections.

- λ_u: mean call initiation rate by a subscriber (calls/busy h/subscriber),
- $1/\mu$: mean call duration (h),
- $1/\eta$: mean subscriber residual time (h),
- v: mean speed at which a subscriber moves in a cell (m/h),
- N: number of channels allocated to a cell,
- U: subscriber density (subscribers/m^2),
- $L(r)$: boundary length of a cell of radius r (m),
- $A(r)$: area covered by a cell of radius r (m^2).

4. Model description

Since the system is assumed to be homogeneous, due to symmetry, we restrict our attention to the flow of calls with respect to a single cell. The single cell has been the unit of analysis in a variety of models under different assumptions [6,14,17,20,21]. One of the advantages of such an approach is that some of the results based on single cell models can provide interesting insights and form the basis for developing models based on multicells.

Without loss of generality, consider a seven-cell cluster consisting of a central cell (the focus of the model) surrounded by six adjacent cells. The following types of calls are considered with respect to the central cell: calls which originate within the cell (i.e., new calls), calls which terminate within the cell, calls which are handed off to an adjacent

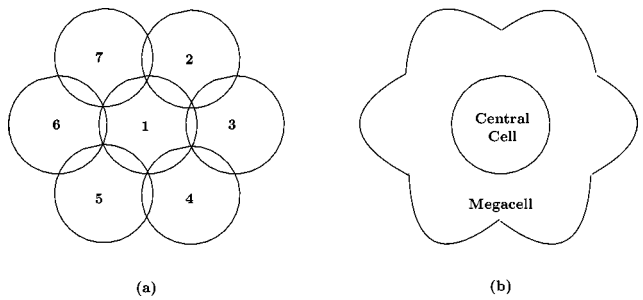

Figure 1. (a) Seven-cell cluster model and (b) aggregate model.

cell from the given cell, and calls which are handed off from an adjacent cell to the given cell.

Let α denote the handoff rate per ongoing call from the central cell to an adjacent cell. Let β denote the handoff rate per ongoing call from an adjacent cell to the central cell. While μ is an input parameter, η depends on the speed of the subscriber, the area of the cell, and the length of the cell boundary. When the system is in a state of mobility equilibrium, η can be approximated as follows [22,23]:

$$\eta = \frac{vL(r)}{\pi A(r)}. \tag{3}$$

Since the system is assumed to be homogeneous, it follows that $\alpha = \beta = \eta$.

The system described above can be modeled as an open network of queues where the station (queue) in the queueing network corresponds to a cell in the cellular network. The external call arrivals in each station in the queueing network correspond to the new calls initiated within each cell. The N servers in each station correspond to the N channels in each cell. Handoffs are modeled as transitions between stations. If a call arrives and finds that all channels are busy, then it is lost.

One of the major drawbacks of the above approach is that the number of call transitions between cells can be quite large. This is because there are two types of call transitions: (i) those between the adjacent cells, and (ii) those between the central cell and the adjacent cells. The number of such transitions increases with the number of cells adjacent to the given cell. Moreover, if there are M cells then the corresponding state transition diagram will be M-dimensional. This implies that the queueing network becomes complex and difficult to solve.

To make the problem more tractable, an aggregate model is used as an approximation as shown in figure 1. Thus, the above system can be modeled as a two-station open queueing network. Station 1 corresponds to a central cell with a capacity of N channels. Station 2 corresponds to a megacell which consists of an aggregation of the six cells adjacent to the central cell. The capacity of station 2 is $6N$ channels. Let λ denote the mean call initiation rate at station 1 where $\lambda = \lambda_{\mathrm{u}} U A(r)$. Then, the mean call initiation rate at station 2 will be 6λ.

One of the major consequences of the above approximation is that internal handoffs between cells which compose the megacell do not have to be captured and only handoffs from and to the central cell will have to be considered. Thus, there are likely to be more handoffs to the central cell than in reality. This implies that there is likely to be more demand for channels and, hence, a greater likelihood of lost calls in the central cell. So, the corresponding model is likely to yield a conservative estimate of the actual performance. From the above reasoning, it can be seen that even though the above model is only an approximation, it can be helpful in providing insights about the impact of mobility on system performance.

5. Analysis

Let k_i $(i = 1, 2)$ denote the number of calls in progress in cell i at steady state, where cell 1 and cell 2 refer to the central cell and the megacell, respectively. Let S_{k_1,k_2}, $0 \leqslant k_1 \leqslant N$ and $0 \leqslant k_2 \leqslant 6N$, denote the steady state. Associated with each state S_{k_1,k_2} is a probability p_{k_1,k_2} which denotes the steady state probability of finding k_1 and k_2 calls in progress in cells 1 and 2, respectively. There are $(N+1)(6N+1) = 6N^2 + 7N + 1$ states of the system.

The state transition diagram is two-dimensional since calls may be in progress in the two cells. In general, given a state S_{k_1,k_2}, the possible transitions to another state are as follows:

1. $S_{k_1,k_2} \to S_{k_1+1,k_2}$ due to a new call arrival in cell 1.
2. $S_{k_1,k_2} \to S_{k_1-1,k_2}$ due to a call completion in cell 1.
3. $S_{k_1,k_2} \to S_{k_1,k_2-1}$ due to a call completion in cell 2.
4. $S_{k_1,k_2} \to S_{k_1,k_2+1}$ due to a new call arrival in cell 2.
5. $S_{k_1,k_2} \to S_{k_1-1,k_2+1}$ due to a call handoff from cell 1 to cell 2.
6. $S_{k_1,k_2} \to S_{k_1+1,k_2-1}$ due to a call handoff from cell 2 to cell 1.

The transitions involving boundary states are shown in figure 2 while the transitions involving interior states are shown in figure 3. From these diagrams, it can be seen that the service rate as well as the handoff rate varies as a linear function of the number of calls in progress. From the state-transition diagram, the balance equations associated with each state can be written. For a given state, the balance equation indicates that under equilibrium conditions in steady state, due to conservation of flow, the total flow out of that state is equal to the total flow into that state.

First, consider the balance equations for the states at the *corners* of the state-transition diagram. For state S_{00}, the balance equation is

$$p_{00}(7\lambda) = \mu p_{01} + \mu p_{10}. \tag{4}$$

For state $S_{N,0}$, the balance equation is

$$p_{N,0}(N\mu + 6\lambda + N\alpha) = \lambda p_{N-1,0} + \beta p_{N-1,1} + \mu p_{N,1}. \tag{5}$$

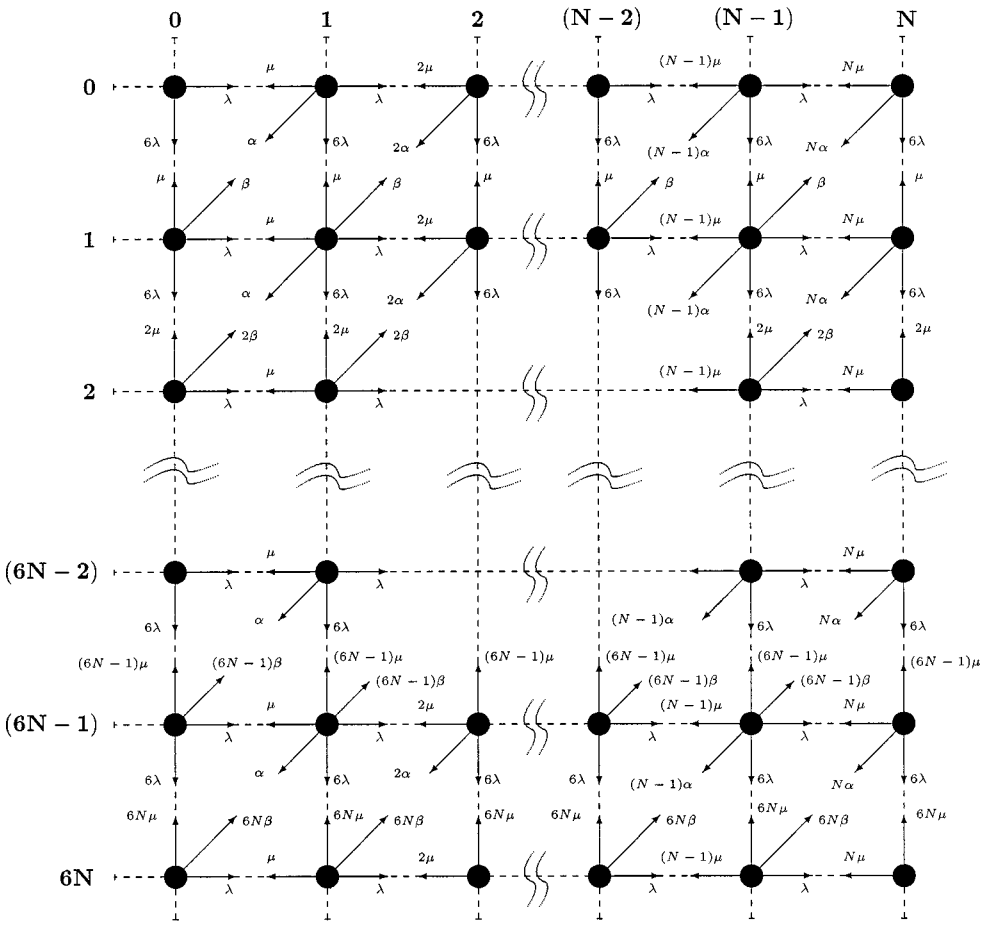

Figure 2. State transition diagram showing boundary states.

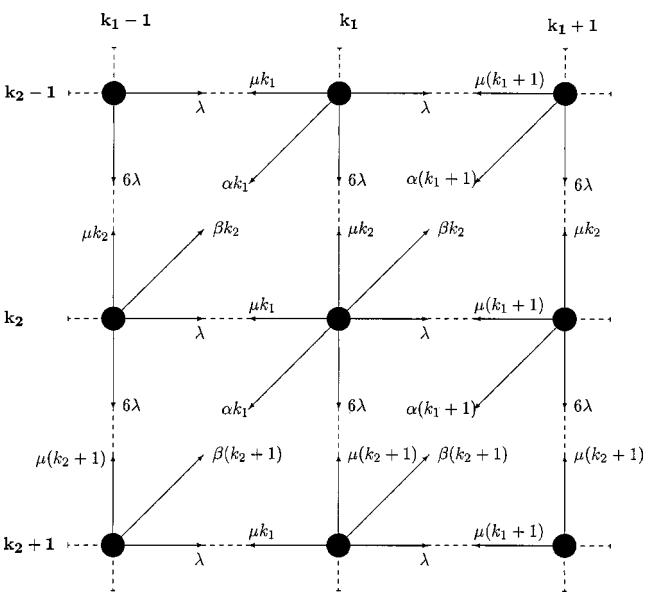

Figure 3. State transition diagram showing interior states.

For state $S_{0,6N}$, the balance equation is

$$p_{0,6N}[6N\mu+6N\beta+\lambda] = 6\lambda p_{0,6N-1}+\alpha p_{1,6N-1}+\mu p_{1,6N}. \tag{6}$$

For state $S_{N,6N}$, the balance equation is

$$p_{N,6N}(7N\mu) = \lambda p_{N-1,6N} + 6\lambda p_{N,6N-1}. \tag{7}$$

For states along the *upper boundary* of the state-transition diagram (i.e., $S_{k_1,0}$ for $1 \leqslant k_1 \leqslant N-1$), the system of balance equations are

$$\begin{aligned} &p_{k_1,0}[k_1\mu + 7\lambda + k_1\alpha] \\ &\quad = \lambda p_{k_1-1,0} + \beta p_{k_1-1,1} + \mu p_{k_1,1} + (k_1+1)\mu p_{k_1+1,0}. \end{aligned} \tag{8}$$

For states along the *lower boundary* of the state-transition diagram (i.e., $S_{k_1,6N}$ for $1 \leqslant k_1 \leqslant N-1$), the system of balance equations are

$$\begin{aligned} &p_{k_1,6N}\big[(6N+k_1)\mu + 6N\beta + \lambda\big] \\ &\quad = \lambda p_{k_1-1,6N} + 6\lambda p_{k_1,6N-1} + (k_1+1)\alpha p_{k_1+1,6N-1} \\ &\qquad + (k_1+1)\mu p_{k_1+1,6N}. \end{aligned} \tag{9}$$

For states along the *left boundary* of the state-transition diagram (i.e., S_{0,k_2} for $1 \leqslant k_2 \leqslant 6N-1$), the system of balance equations are

$$\begin{aligned} &p_{0,k_2}[k_2\mu + k_2\beta + 7\lambda] \\ &\quad = 6\lambda p_{0,k_2-1} + \alpha p_{1,k_2-1} + \mu p_{1,k_2} + (k_2+1)\mu p_{0,k_2+1}. \end{aligned} \tag{10}$$

For states along the *right boundary* of the state-transition diagram (i.e., S_{N,k_2} for $1 \leqslant k_2 \leqslant 6N-1$), the system of balance equations are

$$\begin{aligned} &p_{N,k_2}\big[(k_2+N)\mu + 6\lambda + N\alpha\big] \\ &\quad = \lambda p_{N-1,k_2} + 6\lambda p_{N,k_2-1} + (k_2+1)\mu p_{N,k_2+1} \\ &\qquad + (k_2+1)\beta p_{N-1,k_2+1}. \end{aligned} \tag{11}$$

For the remaining states of the state transition diagram (i.e., S_{k_1,k_2} for $1 \leqslant k_1 \leqslant N-1$ and $1 \leqslant k_2 \leqslant 6N-1$), the system of balance equations are

$$\begin{aligned} &p_{k_1,k_2}\big[(k_1+k_2)\mu + k_2\beta + 7\lambda + k_1\alpha\big] \\ &\quad = \lambda p_{k_1-1,k_2} + 6\lambda p_{k_1,k_2-1} \\ &\qquad + (k_1+1)\alpha p_{k_1+1,k_2-1} + (k_1+1)\mu p_{k_1+1,k_2} \\ &\qquad + (k_2+1)\mu p_{k_1,k_2+1} + (k_2+1)\beta p_{k_1-1,k_2+1}. \end{aligned} \tag{12}$$

The final balance equation is

$$\sum_{k_1=0}^{N}\sum_{k_2=0}^{6N} p_{k_1k_2} = 1. \tag{13}$$

One of the major challenges in performing the computational experiments is the determination of the steady-state probabilities p_{k_1,k_2}, where $0 \leqslant k_1 \leqslant N$ and $0 \leqslant k_2 \leqslant 6N$. These values can be determined by solving $(6N^2+7N+1)$ linear equations. The input matrix for the above problem is of size $m \times m$ where $m = 6N^2+7N+1$, and can become quite large as N increases. This makes the problem difficult to solve in a reasonably short time.

The first step is to solve the system of linear equations given by $\mathbf{Ax} = \mathbf{b}$, where $\mathbf{A}$ denotes the input matrix, $\mathbf{x}$ denotes the vector (of size m) of steady-state probabilities, and $\mathbf{b}$ denotes the right-hand side vector (of size m). $\mathbf{A}$ contains the coefficients of the steady-state probabilities in the system of linear equations; $\mathbf{x} = (x_t)$, where $x_t = p_{k_1,k_2}$ and $t = (N \cdot k_2) + (k_1 + k_2 + 1)$; and $\mathbf{b} = (0, 0, \ldots, 0, 1)$. The unit value in vector $\mathbf{b}$ corresponds to the right-hand side of equation (13). Since $\mathbf{b} \neq 0$, the above system of linear equations is inhomogeneous.

The input matrix $\mathbf{A}$ has a special structure: it is nonsymmetric and sparse. The sparsity follows from the fact that the transitions are restricted to the neighboring states. From equation (13), all elements of the bottom row of $\mathbf{A}$ will be 1. It follows from above that the structure of $\mathbf{A}$ is "banded with single border". This special structure of the matrix was exploited in obtaining the steady-state probabilities.

For example, it was found that, for a given value of N, the number of nonzero elements in $\mathbf{A}$ is $48N^2+28N-1$ (as opposed to $36N^4+84N^3+61N^2+14N+1$ if the matrix was dense). Thus, the required storage can be reduced by about two orders of magnitude, if only the nonzero elements are stored. A *triad* format was used to store only the nonzero elements of matrix $\mathbf{A}$. The nonzero elements were stored in an arbitrary order as a set of triples (a_{ij}, i, j).

A library of subroutines [24] based on Gaussian elimination and pivotal interchanges along with iterative refinement was used to obtain the steady-state probabilities. The procedure was coded in Fortran and the experiments were run on a Silicon Graphics workstation. Estimates of accuracy were obtained by inspection of the max-norm of the last correction vector, the max-norm of the last residual vector, and the growth factor.

6. Determining performance measures

Given that the the steady-state probabilities p_{k_1,k_2} where $0 \leqslant k_1 \leqslant N$ and $0 \leqslant k_2 \leqslant 6N$ have been determined, the next step is to determine the performance measures which will help in configuring the cellular network. Examples of such measures include the carried traffic due to new calls, the carried traffic due to handoff calls in the central cell, and the incoming handoff traffic which is blocked in the central cell. These measures can be subsequently used to determine the expected net revenues.

Let Q_{N} denote the carried traffic (in calls/h/cell) due to new calls and Q_{H} the carried traffic due to handoff calls in the central cell (i.e., cell 1). Then,

$$\begin{aligned} Q_{\mathrm{N}} = &\big[\lambda(p_{00} + p_{10} + \cdots + p_{N-1,0})\big] \\ &+ \big[\lambda(p_{01} + p_{11} + \cdots + p_{N-1,1})\big] + \cdots \\ &+ \big[\lambda(p_{0,6N} + p_{1,6N} + \cdots + p_{N-1,6N})\big]. \end{aligned} \tag{14}$$

From equation (13) it follows that

$$Q_{\mathrm{N}} = \lambda\left(1 - \sum_{j=0}^{6N} p_{Nj}\right). \tag{15}$$

Q_{H} can be determined as follows:

$$\begin{aligned} Q_{\mathrm{H}} = &\big[\beta(p_{01} + p_{11} + \cdots + p_{N-1,1})\big] \\ &+ \big[2\beta(p_{02} + p_{12} + \cdots + p_{N-1,2})\big] + \cdots \\ &+ \big[6N\beta(p_{0,6N} + p_{1,6N} + \cdots + p_{N-1,6N})\big] \end{aligned} \tag{16}$$

$$= \beta \sum_{i=0}^{N-1}\sum_{j=1}^{6N} j p_{ij}. \tag{17}$$

A handoff call attempted from adjacent cells (cell 2) to the central cell (cell 1) is blocked if all N channels in the given cell are busy. The states $p_{N,j}$, $j = 1, \ldots, 6N$, along the right boundary of the state transition diagram in figure 2, represent the events where all N channels are busy in the given cell and there exists at least one call in progress in the adjacent cells. Taking into account the dependence of handoff rates on the number of active calls, the mean number of handoff calls per unit of time trying to move into the central cell but are blocked is

$$B_{\mathrm{H}} = \beta \sum_{j=1}^{6N} j p_{N,j}. \tag{18}$$

As explained earlier, one of the consequences of aggregating adjacent cells into a megacell is that the handoffs between the adjacent cells are ignored. Besides, the capacity

of the megacell is much higher. Due to trunking efficiencies obtained from pooling of channels, it follows that handoffs from the central cell to the megacell are less likely to be blocked. The corresponding performance of the megacell is likely to be an overestimate of the actual performance. For the above reasons, the computations related to handoff traffic to the megacell are not considered.

Other performance measures which are of interest to the system designer include the following: B_N ($= \lambda - Q_N$) is defined as the mean number of blocked new calls per hour per cell; P_C ($= 100 \cdot Q_H/[Q_N + Q_H]$) is the mean handoff traffic carried in the given cell as a percentage of the total carried traffic; P_N ($= B_N/[Q_N + B_N]$) is the blocking probability of new calls; and P_H ($= B_H/[Q_H + B_H]$) is the blocking probability of handoff calls.

7. Experimental design

This section contains a brief description of the various experiments in terms of input parameters, objectives, and output measures. The formulae presented in the previous section were used to determine the output measures.

The values of the input parameters were selected based on interviews with cellular companies and based on previously published research [12,13,15,18,19]. They include the following: $U = 0.0001$ subscribers/m^2, $1/\mu = 2.0$ min. The values for the mean call initiation rate were chosen to be 0.1, 1.0 and 2.0 calls/h/subscriber to represent low, medium and high traffic, respectively. The values for the mean speed of subscriber mobility were chosen to be 5 km/h ($\approx$3 miles/h) to represent low mobility (e.g., pedestrian traffic), 40 km/h ($\approx$25 miles/h) to represent medium mobility (e.g., in residential areas), and 90 km/h ($\approx$55 miles/h) to represent high mobility (e.g., freeway traffic). In addition, the case of no mobility (i.e., 0 km/h) was also studied.

Three sets of experiments were done. The first set of experiments investigated the effect of subscriber mobility when the mean call initiation rate was low. λ_u was set to 0.1 calls/h/subscriber and a different run was performed for each value of subscriber speed v (i.e., 0, 5, 40 and 90 km/h). The second and the third set of experiments were similar to the first set, except that λ_u was set to 1.0 and 2.0, respectively. Given λ_u, v and N, each experiment included the generation of the input matrix, determination of the steady-state probabilities, and the computation of specific performance measures for cell radius ranging from 50 to 6000 m, in increments of 50 m. The above sets of experiments were repeated for two different channel capacities: $N = 10$ and 50.

In each experiment, the values of the following performance measures were computed: the carried traffic due to new calls (Q_N), the carried traffic due to handoff calls in the central cell (Q_H), and the incoming handoff traffic which is blocked in the central cell (B_H). These values were, in turn, used to determine the mean number of blocked new calls per hour per cell (B_N), the mean handoff traffic carried in the given cell as a percentage of the total carried traffic (P_C), the blocking probability of new calls (P_N), and the blocking probability of handoff calls (P_H).

8. Computational results

The steady-state probabilities obtained by solving the system of linear equations for different experiments had a relative error of 10^{-7}–10^{-9}. The number of iterations required to solve the system of linear equations varied from 3 to 5. The average time for the completion of each experiment was about 52 s for $N = 10$, while it was about 3.6 h (i.e., about 108 s for a given cell radius) for $N = 50$. The higher time for the latter was due to the larger state space.

Some of the major results from the experiments are described below. In the following discussion, r^* denotes a cutoff value of cell radius at which system behavior tends to change. This notation is used for convenience and the actual value of r^* may not be the same for all cases. Besides, $\lambda(r)$ is used interchangeably with λ to emphasize that λ is a function of cell radius r.

First, the impact of varying the cell size (i.e., increasing the transmission power of base stations and subscriber terminals thereby increasing the cell radius) is presented (see figures 4–8). The values of other input parameters (λ_u, v and N) were kept constant.

1. *As cell radius increases, the blocking probability of new calls (P_N) is zero until $r \leqslant r^*$, after which it increases at a rapid rate.* As cell radius increases, $\lambda(r)$ also increases. Initially, the available channel capacity N is sufficient to accommodate the increase in $\lambda(r)$, resulting in no blocking of new calls. However, for $r > r^*$, N is not sufficient to handle the traffic. As a result, the blocked new call traffic tends to increase at a rapid rate.

2. *For mobile subscribers (i.e., $v > 0$), as cell radius increases, the carried handoff traffic (Q_H) drastically decreases until $r \leqslant r^*$, after which it gradually decreases*

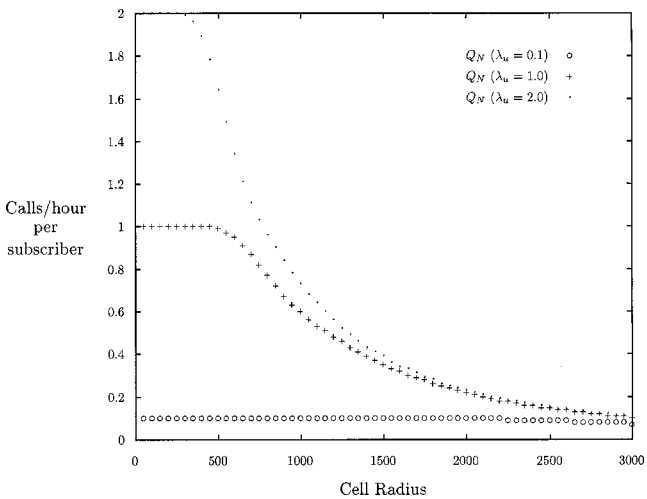

Figure 4. Impact of cell size on carried new call traffic Q_N ($N = 10$, $v = 5$ km/h).

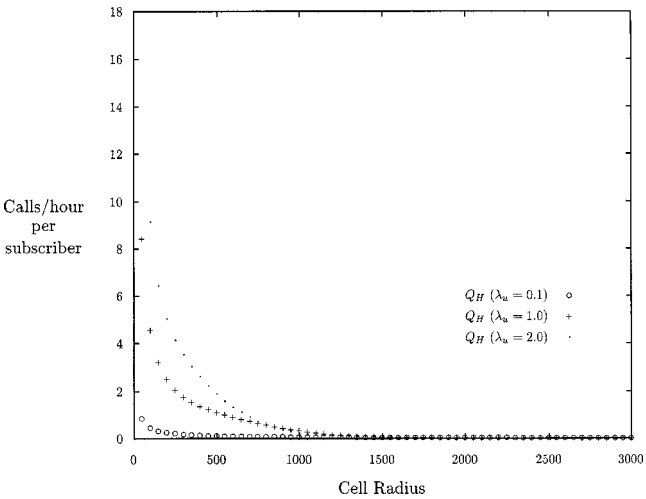

Figure 5. Impact of cell size on carried handoff traffic Q_{H} ($N = 10$, $v = 5$ km/h).

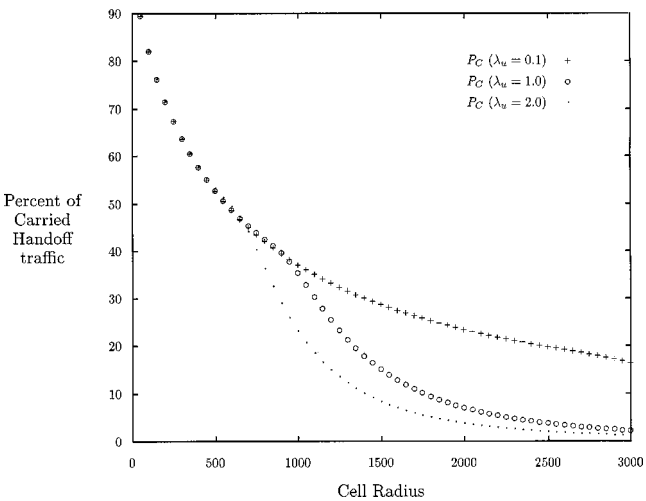

Figure 6. Impact of cell size on carried handoff traffic as a percent of total carried traffic P_{C} ($N = 10$, $v = 5$ km/h).

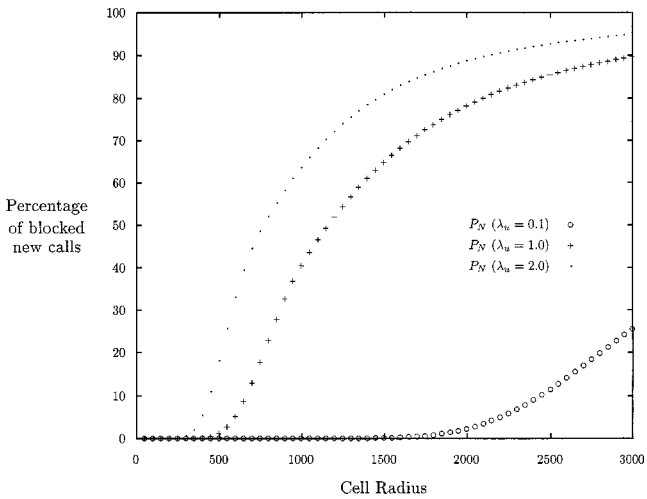

Figure 7. Impact of cell size on blocking probability of new calls P_N ($N = 10$, $v = 5$ km/h).

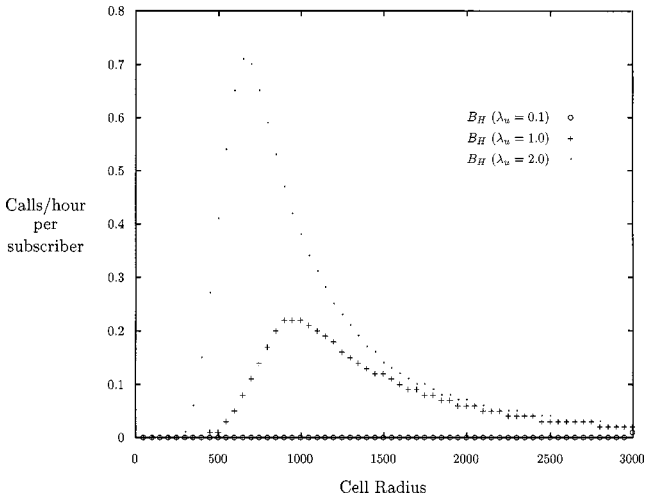

Figure 8. Impact of cell size on blocked handoff traffic B_{H} ($N = 10$, $v = 5$ km/h).

to zero. From equation (3), it follows that $\eta = 2v/\pi r$. Hence, $\eta/\mu = K/r$, where $K = 2v/\pi\mu$. For given input parameters v and μ, K will be a constant, and hence, as cell size increases, η/μ decreases.

Initially, for small cells, $\eta > \mu$, which implies that the likelihood for handoffs is high. Since $\lambda(r)$ is low and the channel capacity N is sufficient, these handoffs are accommodated by the cell. As cells become larger, $\lambda(r)$ increases leading to increased blocking of handoff calls (as can be seen from the peak in the curve for B_{H} in figure 8). For cells beyond a certain size, the blocking of handoff calls decreases. However, the carried traffic due to handoff calls continues to decrease. This apparent paradox can be explained as follows.

As cells become larger, $\eta \leqslant \mu$, and hence, handoffs become less likely. Besides, the new call traffic in adjacent cells becomes larger and the available channel capacity may not be sufficient to handle all the traffic. This results in the increased blocking of new calls in adjacent cells, and hence, fewer handoff calls from the adjacent cells. This follows from the fact that P_{C} and B_{H} tend to decrease for large cells (see figures 6 and 8). Thus, the decrease in carried handoff traffic for $r > r^*$ is due to fewer incoming handoff calls and not due to increase in the blocking of handoff calls.

3. *For mobile subscribers, as cell radius increases, the carried handoff traffic (Q_{H}) exceeds the carried new call traffic (Q_{N}) for $r \leqslant r^*$. However, for larger cells, $Q_{\mathrm{H}} < Q_{\mathrm{N}}$.* In general, the aggregate traffic in adjacent cells is greater than the traffic in the given cell. Besides, for small cells with radius less than r^*, there is greater likelihood of handoff to the given cell since subscribers can reach the cell boundary quickly. In addition, due to small cell sizes, $\lambda(r)$ tends to be relatively small. Hence, $Q_{\mathrm{H}} > Q_{\mathrm{N}}$ for small cells. However, for large cells, as explained above, the carried traffic due to handoff calls tends to decrease due to fewer handoffs. This behavior also follows from the fact that for small cells, the carried

handoff traffic as a fraction of total carried traffic (P_C) is higher than 50% (see figure 6); however, for larger cells, P_C is lower than 50% and tends to decrease.

The impact of varying cell size on the blocking probability of handoff calls (P_H) is similar to that on the blocking probability of new calls (P_N) (see figure 7), and hence, the corresponding figure is not shown. However, one of the interesting findings of the above experiments is that reliance on P_H alone can be misleading. Thus, beyond a certain cell size, P_H increases at a rapid rate with increase in cell radius. If this behavior is considered independently, one may erroneously conclude that use of large cells may lead to excessive blocking of handoff calls. However, this conclusion is not necessarily true when the behavior of blocked handoff traffic (see figure 8) is considered in conjunction with that of P_H. The reason for the above behavior of P_H is that, for reasonably large cells, the total offered handoff traffic decreases at a faster rate than the decrease in the blocked handoff traffic.

In general, the above results remain valid for a higher value of λ_u except that r^* tends to be lower. This is because the offered traffic due to new calls tends to be higher in each cell, and hence, the demand for channels tends to be higher. So, available resources (channels) tend to be consumed faster leading to a significant change in system behavior at relatively small cell sizes.

Another difference is with respect to the value of carried handoff traffic (Q_H). For small cells, $Q_H(\lambda_u = 2.0) > Q_H(\lambda_u = 1.0) > Q_H(\lambda_u = 0.1)$. However, for medium to large cells, the inequality in the above expression is reversed. This is because, for large cells, the blocked handoff traffic B_H tends to be higher, and consequently, P_C tends to be lower as λ_u increases. This implies that the increase in λ_u has a significant impact on the handoff traffic for medium to large cells.

On the other hand, if a higher value of N is used (while λ_u and v are constant), the results remain similar except that r^* tends to be higher. The availability of more channels implies that more calls can be accommodated for a given cell radius. Since λ_u is constant, this implies that traffic from relatively larger cells can be accommodated. Hence, r^* tends to be higher.

The impact of varying subscriber mobility (i.e., v) is presented below (see figures 9–13). The values of other input parameters (λ_u, r and N) were kept constant.

1. *For $r < r^*$, the carried traffic due to new calls (Q_N) is independent of v.* This follows from the fact that for $r < r^*$, $P_N = P_H = 0$. This is because $\lambda(r)$ is small for small values of cell radius. So, the channels assigned to the cell are sufficient to handle all the traffic due to new calls as well as handoff calls. Increase of v tends to increase the amount of handoff traffic. However, this increase can be fully absorbed by the available channel capacity for $r < r^*$, and hence, Q_N is not affected. If λ_u is increased further, r^* tends to decrease.

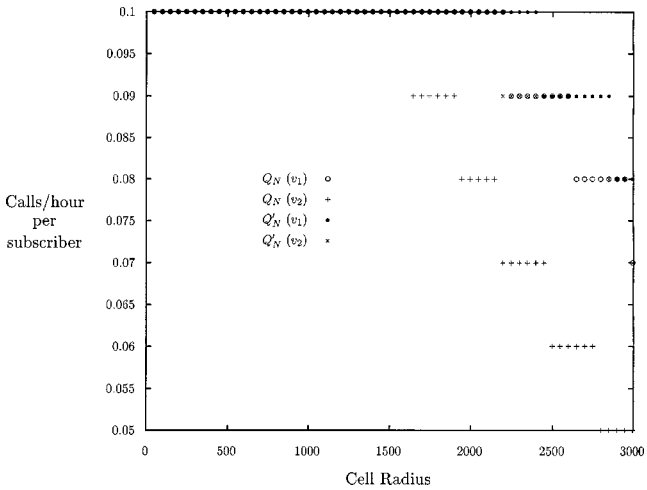

Figure 9. Impact of subscriber mobility on carried new call traffic: method 1 versus method 2 ($N = 10$, $\lambda_u = 0.1$, $v_1 = 5$ km/h, $v_2 = 40$ km/h).

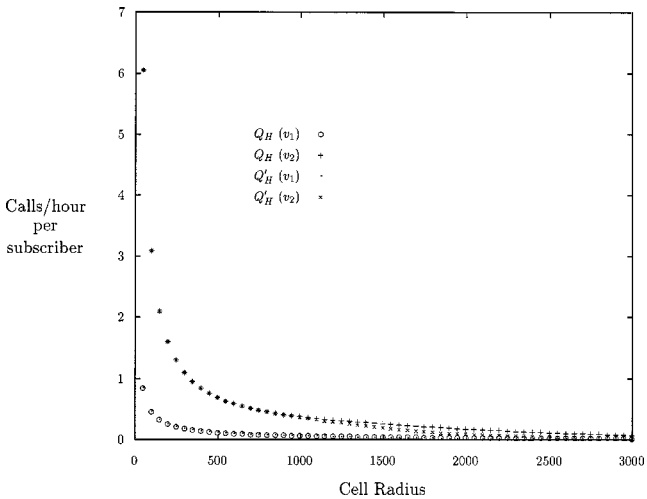

Figure 10. Impact of subscriber mobility on carried handoff traffic: method 1 versus method 2 ($N = 10$, $\lambda_u = 0.1$, $v_1 = 5$ km/h, $v_2 = 40$ km/h).

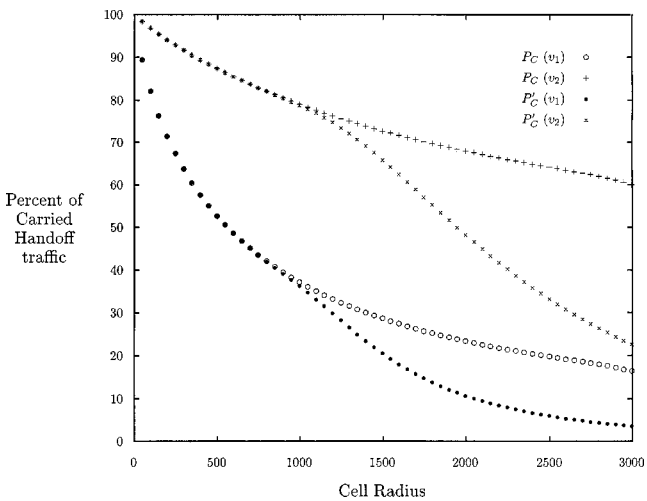

Figure 11. Impact of subscriber mobility on carried handoff traffic as a fraction of the total carried traffic: method 1 versus method 2 ($N = 10$, $\lambda_u = 0.1$, $v_1 = 5$ km/h, $v_2 = 40$ km/h).

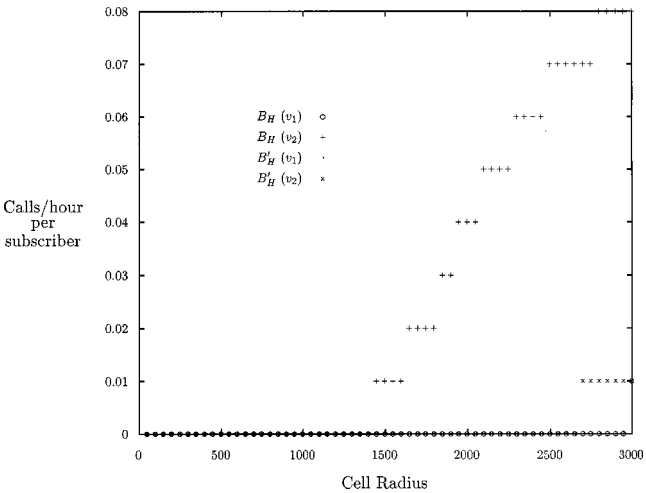

Figure 12. Impact of subscriber mobility on blocked handoff traffic: method 1 versus method 2 ($N = 10$, $\lambda_u = 0.1$, $v_1 = 5$ km/h, $v_2 = 40$ km/h).

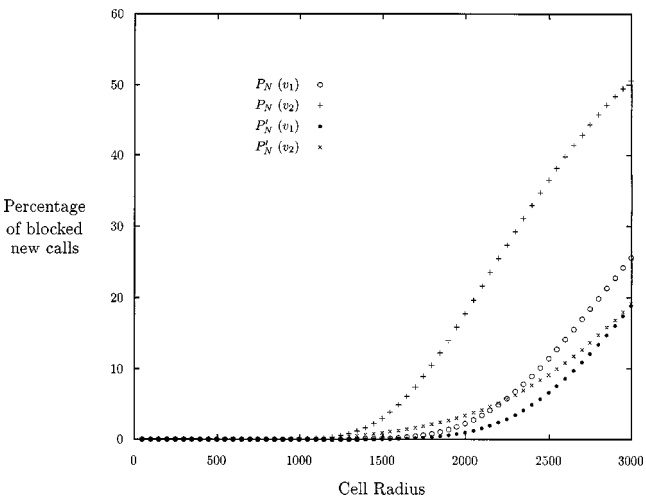

Figure 13. Impact of subscriber mobility on the blocking probability of new calls: method 1 versus method 2 ($N = 10$, $\lambda_u = 0.1$, $v_1 = 5$ km/h, $v_2 = 40$ km/h).

2. *For $r > r^*$, as v increases, Q_N tends to decrease*. This is because the traffic due to handoff calls tends to increase with v. Since the cell size remains unchanged, the new call traffic initiated in the cell remains the same while the handoff traffic from adjacent cells increases. The cell is, therefore, likely to accomodate more handoff traffic than new call traffic. Thus, the increase in Q_H tends to be at the expense of Q_N. This behavior is confirmed by the increase in P_C with increase in v (see figure 11). Moreover, for larger cells, $\lambda(r)$ also becomes large. As a result, the available channel capacity may not be sufficient to carry the traffic, resulting in the increase of P_N, and hence, in the decrease of Q_N (see figure 13).

3. *For $r > r^*$, as v increases, the blocked handoff traffic (B_H) tends to increase*. This is because as v increases, the likelihood of handoffs also increases. For large cells, the new call traffic generated in the cell is also high. If the cell size exceeds a certain value, then most of the available channels in the cell tend to be busy leading to increased blocking of handoff traffic (see figure 12).

9. Comparison with traditional method

As explained in section 2, the handoff rate used in the proposed model varies as a linear function of the number of calls in progress in the cell. In this section, we compare the results of the above method (denoted as method 1) with the traditional method (denoted as method 2) of modeling handoffs using information about the average behavior.

In method 2, the handoff attempts are modeled by assuming a fixed probability θ_{ij} of call transitions from cell i to cell j [2,11]. To make the comparison meaningful, the system is modeled as a two-station queueing network, where station 1 corresponds to the central cell and station 2 corresponds to an aggregation of the six cells adjacent to the central cell.

Let e_j denote the total arrival rate of calls (new as well as handoff) to cell j. Let $\rho_j = e_j/(\eta+\mu)$ and $B_j = E(\rho_j, C_j)$ where $E(\cdot,\cdot)$ is the Erlang loss function and $C_1 = N$ and $C_2 = 6N$. Let $\theta = \eta/(\eta+\mu)$. Since the system is assumed to be homogeneous, $\theta_{ij} = \theta_{ji} = \theta$. Let $\lambda_1 = \lambda$ and $\lambda_2 = 6\lambda$. Then, under equilibrium conditions, the following system of equations needs to be solved:

$$e_i = \lambda_i + e_j(1 - B_j)\theta, \quad i = 1, 2;\ j \neq i. \tag{19}$$

Let Q'_N, Q'_H, B'_H, B'_N, P'_C, P'_N and P'_H denote the performance measures similar to Q_N, Q_H, B_H, B_N, P_C, P_N and P_H (see section 6), respectively. Then, by definition,

$$Q'_N = \lambda(1 - B_1), \tag{20}$$

$$Q'_H = e_2(1 - B_2)\theta(1 - B_1), \tag{21}$$

$$B'_H = e_2(1 - B_2)\theta B_1. \tag{22}$$

The expressions for P'_C, P'_N and P'_H will be the same as for P_C, P_N and P_H, respectively.

The same sets of experiments as described in section 7 were done for method 2. The initial values for B_1 and B_2 were set to 0.0. Then, using fixed point iteration, the actual values of B_i, $i = 1, 2$, were found. The iterations were stopped when the number of iterations exceeded 100000 or if the B_i values between two consecutive iterations did not differ by more than 10^{-10}. Except for five instances, fewer than 100 iterations were required for the B_i values to converge.

When there was no subscriber mobility (i.e., $v = 0$), the results yielded by the two methods were identical. When the subscribers were mobile (i.e., $v > 0$), the structure of the solutions in terms of the impact of cell size, mean call initiation rate, the number of channels and mobility on the performance measures were the same. However, the results differed in several respects and are described below. As in section 8, in the following discussion, r^* denotes a cutoff

value of cell radius at which system behavior tends to change and the actual value of r^* may not be the same for all cases.

For a given set of input parameters, the major differences in the results of the two methods are described below (see figures 9–13). Beyond a certain cell size, the carried new call traffic under method 2 is higher than that under method 1 (i.e., $Q'_{\mathrm{N}} > Q_{\mathrm{N}}$). However, in terms of the other performance measures, for cells beyond a certain size, method 2 yields lower values than method 1 (i.e., $Q'_{\mathrm{H}} < Q_{\mathrm{H}}$, $P'_{\mathrm{C}} < P_{\mathrm{C}}$, $P'_{\mathrm{N}} < P_{\mathrm{N}}$, $B'_{\mathrm{H}} < B_{\mathrm{H}}$). The above results imply that when subscribers are mobile, beyond a certain cell size, method 2 tends to underestimate the handoff traffic (blocked as well as carried) than under method 1. Besides, the variance in the results tends to increase with cell size and with mobility. The above findings remain valid even for higher values of λ_{u}.

In general, mobility imposes a cost in terms of requiring additional channels to meet a required blocking probability [3], and this cost tends to increase with mobility. Method 2, as explained above, tends to underestimate this cost and hence the corresponding results may not be accurate. Method 1 provides a more reliable measure of this cost since it accounts for additional handoff traffic by making the handoff rates dependent on the active number of calls in adjacent cells.

10. Economic impact

In this section, the economic impact of mobility on system configuration decisions is explored. Several experiments are done to determine the optimal cell size and the optimal number of channels required at different values of subscriber mobility and call initiation rates.

A similar study was done in an earlier paper [4]. However, subscriber mobility was ignored. The study presented in this section explicitly takes into account the impact of subscriber mobility. Another difference between this study and the earlier study [4] is in terms of computation of R_{h}, the total call revenue per busy hour. R_{h} is used to determine the net revenue corresponding to a given system configuration. To determine R_{h}, it is necessary to determine T, the mean number of calls carried in a cell (i.e., cell 1 in our case) per unit of time. The procedure for determining T is given below.

Given the carried traffic due to new calls (Q_{N}) and the carried traffic due to handoff calls (Q_{H}) in the central cell, the mean number of calls carried by the central cell per unit of time is

$$T = Q_{\mathrm{N}} + Q_{\mathrm{H}}. \tag{23}$$

Let R_{f} denote the charge for the first minute of call and R_{o} denote the charge per minute for subsequent minutes. Then, the corresponding call revenue per hour per cell is

$$R_{\mathrm{h}_1} = T\left[R_{\mathrm{f}} + \left\lceil \frac{1}{\mu} - 1 \right\rceil^{+} R_{\mathrm{o}}\right]. \tag{24}$$

It is a common practice in the cellular industry to offer credit to subscribers whose calls have been abruptly terminated due to blocked handoff calls. This is because subscribers are more sensitive to abrupt termination of ongoing calls than to getting a busy tone during call initiation. The amount of credit depends on several factors such as the length of the call before it was terminated, the importance attached to such disruptions by the service provider, and regulatory requirements. For convenience, assume that the amount of credit corresponds to the revenue obtained during the average length of the call. The issue of credit results in a loss of revenue to the service provider. The amount of loss in revenue per hour per cell is

$$R_{\mathrm{h}_2} = B_{\mathrm{H}}\left[\frac{1}{\mu} R_{\mathrm{o}}\right]. \tag{25}$$

From (24) and (25), the total call revenue per hour per cell is

$$R_{\mathrm{h}} = R_{\mathrm{h}_1} - R_{\mathrm{h}_2}. \tag{26}$$

Let h_{day} denote the number of busy hours per day and let Y denote the number of business days per year. Then, the annual call revenue for a cell of radius r and i channels is

$$R_{\mathrm{call}}(i, r) = R_{\mathrm{h}} h_{\mathrm{day}} Y. \tag{27}$$

Let R_{co} denote the connect charges from subscribers (\$/month) and $M(r) = \lceil A/A(r) \rceil$. Then, the expected annual revenues for the entire service area is

$$R_{\mathrm{tot}}(i, r) = M(r) R_{\mathrm{call}}(i, r) + R_{\mathrm{ct}}, \tag{28}$$

where $R_{\mathrm{ct}} = R_{\mathrm{co}} \cdot U \cdot A \cdot 12$.

The next step in determining the net revenue is to determine the total costs. The major cost components are the cost of setting up and maintaining the tower and the cost of channels in each cell. Let

- T: number of tower types,
- t^*: optimal tower type,
- $D(t)$: maximum radius covered by tower of type t (m),
- $C_{\mathrm{tr}}(t)$: annualized set-up cost of tower type t (\$),
- $C_{\mathrm{mt}}(t)$: annual maintenance and operations cost of tower type t (\$),
- $C_{\mathrm{ch}}(t)$: channel cost associated with tower type t (\$).

When tower type t with i channels is used, the annual cost per cell is

$$C(i, t) = C_{\mathrm{tr}}(t) + C_{\mathrm{mt}}(t) + i C_{\mathrm{ch}}(t). \tag{29}$$

Hence, for a network of cells of radius r with i channels assigned to each cell, the expected annual costs for the service area are given by

$$C_{\mathrm{tot}}(t, i, r) = M(r) C(i, t). \tag{30}$$

Given the expected annual revenues and the annual costs for the cellular network, it is straightforward to compute the expected annual net revenues. For a cellular network of $M(r)$

Table 1
Input parameters associated with towers.

Tower type	Tower range cost (in m)	Setup cost (in \$)	Channel cost (in \$/year)	Mtce./Opns. cost (in \$/year)
1	300	20,000	300	2,500
2	800	150,000	500	20,000
3	1,500	500,000	500	40,000
4	3,000	1,600,000	750	60,000
5	6,000	3,000,000	1,250	100,000

cells, each of which has radius r and uses tower t and i channels, the expected annual net revenues are given by

$$NR(t, i, r) = R_{\text{tot}}(i, r) - C_{\text{tot}}(t, i, r). \tag{31}$$

The parameters used in this study are as follows:

$$\begin{aligned}
\text{subscriber density} &= 0.0001 \text{ subscribers/m}^2,\\
\text{mean call duration} &= 2.0 \text{ min},\\
\text{available channels} &= 50,\\
\text{service area} &= 1.6 \text{ billion m}^2,\\
\text{subscription charge} &= \$\ 25.00/\text{month},\\
\text{estimated tower life} &= 5 \text{ years},\\
R_{\text{f}} &= \$\ 0.25/\text{first minute},\\
R_{\text{o}} &= \$\ 0.15/\text{minute},\\
h_{\text{day}} &= 6,\\
Y &= 260 \text{ days}.
\end{aligned}$$

The input parameters associated with towers are listed in table 1.

For a given cell radius r, the number of cells required to cover the given service area is determined as $M(r) = \lceil A/A(r) \rceil$. Next, the optimal tower type is chosen after comparing the cell radius r with the range $D(t)$ of each tower t. The tower whose range just exceeds the cell radius r is chosen the optimal tower type t^*. Then, the traffic-related values such as the mean call initiation rate per cell $\lambda(r)$ $(= \lambda_{\text{u}} U A(r))$ and the number of subscribers in the service area S $(= UA)$ are determined. Next, using N available channels in each cell, the net revenues are computed using the procedure outlined above. However, the use of all the available N channels may not necessarily maximize the expected net revenue. Hence, the procedure for determining net revenues is repeated for each value of i, where $1 \leqslant i \leqslant N$. The number of channels which yields the maximum net revenue is chosen as the optimal number of channels (N^*) for each cell.

In the first experiment, the maximum number of channels, N, was set to 50. The cell radius was varied from 50 to 6000 m in increments of 50 m. For a given call initiation rate, λ_{u}, the net revenue for each value of cell radius was determined as described earlier. The above experiment was repeated for different values of λ_{u} (i.e., 0.1 and 1.0 calls/h/subscriber) and for different values of subscriber speed v (i.e., 5 and 40 km/h). The values of other input parameters were kept constant. The results of the above experiments are discussed below.

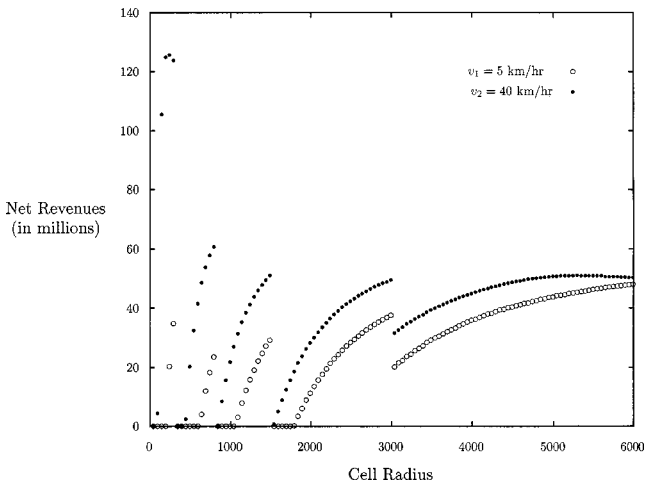

Figure 14. Impact of subscriber mobility on net revenues ($\lambda_{\text{u}} = 0.1$ calls/h/subscriber).

From figure 14, it can be seen that the net revenue has a nonlinear strucuture similar to that of a sawtooth function. Thus, there are large changes in net revenue when cell radius just exceeds 300, 800, 1500 and 3000 m. These large changes in net revenue are due to the changes in the choice of tower used in each cell. In fact, for low values of mean call initiation rate, subscriber speed and cell size, the total costs can exceed the total revenues (note: negative values of net revenues are denoted as points on the x-axis in the figure). Besides, the magnitude of the change in net revenue seems to decrease with increase in cell radius.

If the subscriber speed is increased, while the other parameters are unchanged, the net revenues also increase. The reason for this behavior can be explained as follows: the increased subscriber mobility results in a higher carried traffic – mainly due to increased handoff traffic (see discussion in section 8) – which contributes to higher net revenues. However, as the cells become larger, the difference in net revenues due to a change subscriber mobility tends to become smaller. One of the reasons for this behavior is that the blocked handoff traffic tends to increase (see figure 12) leading to a higher penalty incurred by the service provider in offering credit for blocked handoff calls. Another reason is that the carried new call traffic also tends to decrease with increase in subscriber mobility (see figure 9), which lowers the revenue due to carried traffic. Both of the above reasons lead to a lower impact on net revenues for large cells.

Another impact of higher subscriber mobility is that the optimal cell size is lower. For low values of call initiation

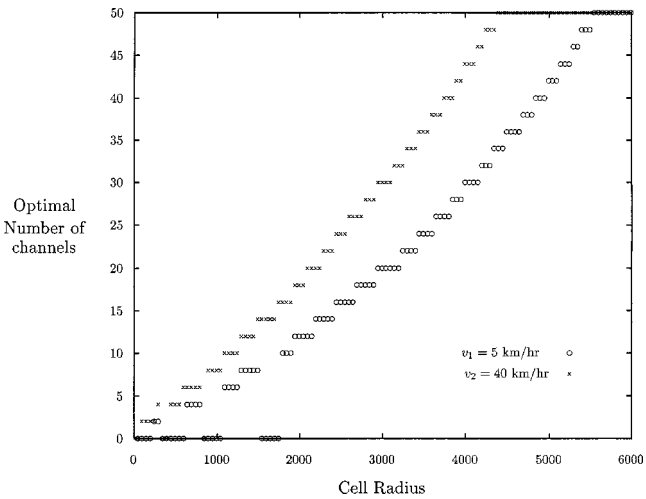

Figure 15. Impact of subscriber mobility on the optimal number of channels ($\lambda_u = 0.1$ calls/h/subscriber).

rate and subscriber mobility, if the cell size is small, it implies that a large number of cells will be required to cover the service area. Since the setup cost of towers, even with small coverage, is relatively high, the revenues due to carried traffic in such a configuration may not justify the necessary investment. However, if the subscriber mobility is high, the carried traffic tends to be higher for small cells. In fact, as cells become larger, the carried traffic tends to decrease as explained in the previous paragraph. Hence, the optimal cell size is lower when subscriber mobility is increased.

Given the mean call initiation rate and subscriber speed, the optimal number of channels which will maximize the expected net revenue tends to increase with cell radius (see figure 15). In the figure, the optimal number of channels is denoted as zero if the corresponding net revenues are negative. This behavior is also true for a higher value of subscriber mobility. However, for a given cell size, if the subscriber speed is increased, the optimal number of channels tends to be higher. Thus, mobility seems to impose a cost in terms of requiring additional number of channels for each cell. This observation is consistent with earlier research [3] on the cost of mobility.

If the mean call initiation rate λ_u is higher, the results remain similar except in terms of the optimal cell size and the optimal number of channels. At a higher λ_u, while other parameters are unchanged, the optimal cell size tends to be lower. Besides, the optimal number of channels required for a given cell size tends to be higher due to higher traffic in the cell.

11. Conclusion

The purpose of the model described in this paper is to study the dynamics of mobility between a single cell and its adjacent cells. It explicitly incorporates the dependency between the handoff rate and the system state. Extensive computational experiments were done to study the impact of various input parameters on specific performance measures.

Several observations were made regarding the system performance and as to how it is affected by the complex interaction between subscriber mobility, cell size, number of channels and the mean call initiation rate. Another interesting observation was that the reliance on a single performance measure may lead to erroneous conclusions and that it is important to consider several performance measures jointly to study the impact of input parameters.

The above experiments were repeated using the traditional method of modeling handoffs using information about the average behavior. The results of these experiments show that the proposed model, where handoff rates are state-dependent, captures additional traffic due to mobility when compared to the traditional method of modeling handoffs. Additional experiments were also done to study the economic impact of mobility on system configuration decisions. Though an approximation, the above work provides interesting insights about the impact of mobility in configuring cellular networks.

Acknowledgements

We wish to acknowledge the help of Mr. Terry Dison, Contel Cellular, and Mr. Allen Bethel, BellSouth Mobility, for clarifying several technical issues and for providing information related to the operation of cellular networks.

References

[1] C.-J. Chang, T.-T. Su and Y.-Y. Chiang, Analysis of a cutoff priority cellular radio system with finite queueing and reneging/dropping, IEEE/ACM Transactions on Networking 2 (1994) 166–175.

[2] D.E. Everitt, Traffic engineering of the radio interface for cellular mobile networks, Proceedings IEEE (1994) 1371–1382.

[3] G.J. Foschini, B. Gopinath and Z. Miljanic, Channel cost of mobility, IEEE Transactions on Vehicular Technology 4 (1993) 414–424.

[4] B. Gavish and S. Sridhar, Economic aspects of configuring cellular networks, Wireless Networks 1 (1995) 115–128.

[5] W.C. Giffin, *Queueing: Basic Theory and Applications* (Grid, Columbus, OH, 1978).

[6] R.A. Guerin, Channel occupancy time distribution in a cellular radio system, IEEE Transactions on Vehicular Technology 3 (1987) 89–99.

[7] M. Herzberg and D. McMillan, State-dependent control of call arrivals in layered cellular mobile networks, Telecommunication Systems 4 (1993) 365–378.

[8] D. Hong and S.S. Rappaport, Traffic model and performance analysis for cellular mobile radio telephone systems with prioritized and nonprioritized handoff procedures, IEEE Transactions on Vehicular Technology 3 (1986) 77–92.

[9] S.S. Kuek, W.-C. Wong, R. Vijayan and D.J. Goodman, A predictive load-sharing scheme in a microcellular radio environment, IEEE Transactions on Vehicular Technology 4 (1993) 519–525.

[10] Y.-B. Lin, S. Mohan and A. Noerpel, Queueing priority channel assignment strategies for hand-off and initial access for a PCS network, IEEE Transactions on Vehicular Technology 3 (1994) 704–712.

[11] D. McMillan, Traffic modeling and analysis for cellular mobile networks, in: *Proc. of Int. Teletraffic Congress* (1991) pp. 627–632.

[12] G. Naik, Cellular phone rates spark static from users, Wall Street Journal (May 5, 1994) B1.

[13] S. Nanda, Teletraffic models for urban and suburban microcells: Cell sizes and handoff rates, IEEE Transactions on Vehicular Technology 4 (1993) 673–682.

[14] D.L. Pallant and P.G. Taylor, Approximation of performance measures in cellular mobile networks with dynamic channel allocation, Telecommunication Systems 2 (1994) 129–163.
[15] P. Petersen, Positioning PCS on the Telecom landscape, Telephony (December 1993) 26–32.
[16] S.S. Rappaport, The multiple-call hand-off problem in high-capacity cellular communications system, IEEE Transactions on Vehicular Technology 3 (1991) 546–557.
[17] S.S. Rappaport and L.-R. Hu, Microcellular communication systems with hierarchical macrocell overlays: Traffic performance models and analysis, Proc. IEEE 9 (1994) 1383–1397.
[18] D.P. Reed, The cost structure of personal communication services, IEEE Communications Magazine 4 (1993) 102–108.
[19] J. Sarnecki, C. Vinodrai, A. Javed, P. O'Kelly and K. Dick, Microcell design principles, IEEE Communications Magazine 4 (1993) 76–82.
[20] R. Steele and M. Nofal, Teletraffic performance of microcellular personal communication networks, IEE Proceedings-I 4 (1992) 448–461.
[21] S. Tekinay and B. Jabbari, A measurement-based prioritization scheme for handovers in mobile cellular networks, IEEE Journal on Selected Areas in Communications 10 (1992) 1343–1350.
[22] R. Thomas, H. Gilbert and G. Mazziotto, Influence of the movement of the mobile station on the performance of a radio cellular network, in: *Proc. 3rd Nordic Seminar* (September 1988) Paper 9.4.
[23] H. Xie and S. Kuek, Priority handoff analysis, in: *Proc. IEEE Veh. Tech. Conf.* (1993) 855–858.
[24] Z. Zlatev, J. Wasniewski and K. Schaumburg, Y12M: solution of large and sparse systems of linear algebraic equations, in: *Lecture Notes in Computer Science*, Vol. 121 (1981).

B. Gavish. Photograph and biography not available at time of publication.
E-mail: gavishb@mail.cox.smu.edu

S. Sridhar. Photograph and biography not available at time of publication.
E-mail: Suresh_Sridhar@i2.com